JMEPEG (2017) 26:1847–1855
DOI: 10.1007/s11665-017-2596-8

1059-9495/$19.00

Microstructure and Tensile Properties of n-SiCp/Mg-9%Al Composites Prepared by Ultrasonic Assisted Hot Pressing of Powder

Ming Li, Hongxia Wang, Kaibo Nie, Yiming Liu, and Wei Liang

(Submitted June 1, 2016; in revised form February 24, 2017; published online March 8, 2017)

In this paper, the Mg-9%Al alloy reinforced by 5 wt.% SiC nanoparticles was fabricated by hot pressing of powder with ultrasonic vibration under a semi-solid state. The influence of hot-pressing temperature on the microstructure and mechanical properties of the n-SiCp/Mg-9%Al composite was investigated. The results indicated that the density of the composite was increased significantly and the agglomeration of SiC nanoparticles was evidently reduced with the increase in the hot-pressing temperature from 450 to 510 °C. Additionally, the elevated hot-pressing temperature resulted in remarkable grain refinement. However, as the hot-pressing temperature increased to 530 °C, the density decreased and the average grain size increased, which caused a decline in the mechanical properties. The study of the interface between the n-SiCp and the matrix in the nanocomposite suggested that n-SiCp bonded well with the matrix without interfacial activity. The ultimate tensile strength, yield strength and elongation to fracture of the nanocomposites were simultaneously enhanced compared with that of the Mg-9%Al alloy. This improvement could be attributed to obvious grain refinement and the Orowan strengthening mechanism.

Keywords hot pressing of powder, magnesium matrix composite, mechanical properties, microstructure, strengthening mechanism

1. Introduction

Magnesium matrix composites (MMCs) have been received extensive attention as structural materials due to their low density and superior specific properties including strength, creep resistance and damping capacity (Ref 1-6). MMCs were divided into continuous-fiber reinforced magnesium matrix composites, short-fiber or whisker reinforced magnesium matrix composites and particle reinforced magnesium matrix composites (PMMCs) according to the reinforcement type. PMMCs, particularly, are widely used in aerospace and automotive industries, owing to its mechanical improved properties by second processing and its low cost (Ref 7-9).

Generally, SiC particles were selected as reinforcements to reinforce magnesium alloys because no chemical reaction was found in the interface between SiC particles and magnesium alloys in both the manufacturing and the solid solution treatment processes (Ref 10, 11). However, it is shown that the addition of micron-size ceramic particles, in common, reduces the ductility of the matrix although improves strength significantly (Ref 12). Recently, studies have reported that SiC nanoparticles not only increase the yield strength and ultimate tensile strength but also improve the ductility (Ref 13-16).

The processing technique is the key to the fabrication of magnesium matrix nanocomposites with optimized properties. In general, it is extremely challenging for conventional stir casting to distribute and disperse SiC nanoparticles uniformly in magnesium melts because of their large surface-to-volume ratio and their low wettability in metal melts (Ref 17). In addition, it is difficult to apply this fabrication technique to produce SiC nanoparticles reinforced MMCs with high volume fractions, which is important for effectively increasing the strength and elastic modulus. PMMCs are often fabricated by powder metallurgy method, which is time-consuming and costly and may generate high porosity within the composite (Ref 18). Compared with these processing techniques, hot pressing of powder assisted ultrasonic vibration not only has the ability to overcome these shortcomings but also has the advantages of easy molding and low energy consumption. The most important factor is that the materials produced by hot pressing of powder assisted ultrasonic vibration under a semi-solid state have fine grains, which may induce more grain boundaries, a more uniform microstructure and interfaces as well as improve the mechanical properties of the materials (Ref 19).

To the best of our knowledge, open literature reports so far suggested that no systematic attempt has been made to fabricate the SiC nanoparticles reinforced MMCs by hot pressing of powder assisted ultrasonic vibration under a semi-solid state. The hot-pressing temperature has an direct effect on the microstructure and mechanical properties of the MMCs. Accordingly, the experiments described in the present work were designed to synthesize MMCs reinforced with SiC

Ming Li, Hongxia Wang, Kaibo Nie, Yiming Liu, and **Wei Liang**, Shanxi Key Laboratory of Advanced Magnesium based Materials, School of Materials Science and Engineering, Taiyuan University of Technology, Taiyuan 030024, China; and Key Laboratory of Interface Science and Engineering in Advanced Materials, Taiyuan 030024, China. Contact e-mail: wanghxia1217@163.com.

nanoparticles that had been introduced via hot pressing of powder assisted ultrasonic vibration under a semi-solid state. The influence of the hot-pressing temperature on microstructure and mechanical properties was also investigated.

2. Materials and Methods

The chemical composition (wt.%) of the matrix material in this paper is Mg-9%Al, which consists of 91% 100 μm magnesium powder and 9% 25 μm aluminum powder, on average. For reinforcement, 5 wt.% SiC nanoparticles with an average particle size of 50 nm are used. The experiment setup for this study is given in Fig. 1. First, n-SiCp/Mg-9%Al composite powder was mechanically blended and then uniaxially cold compacted at 10 MPa to produce a green billet in the hot-pressing mold. Then, it was heated to the target temperatures of 450, 470, 490, 510 and 530 °C, respectively. The powders were then isothermally held for 20 min. Finally, the powders were pressed at 15 MPa and held for 30 min. During the pressing process, the n-SiCp/Mg-9%Al composite was ultrasonicated from the bottom-up at the same time, as shown in Fig. 1. The ultrasonic vibration device consisted of a transducer with a maximum power of 1 kw and a frequency of about approximately 20 kHz. After that, the resulting rectangular specimen with dimensions of 90 mm × 40 mm × 5 mm, as shown in Fig. 2, was cooled at a rate of 25 °C/min in the die.

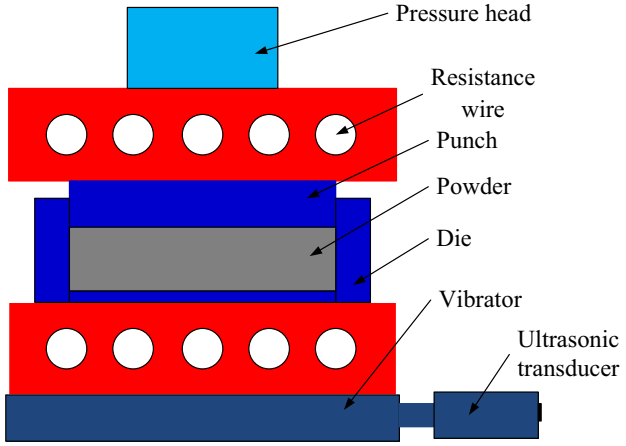

Fig. 1 Schematic diagram of the experimental setup

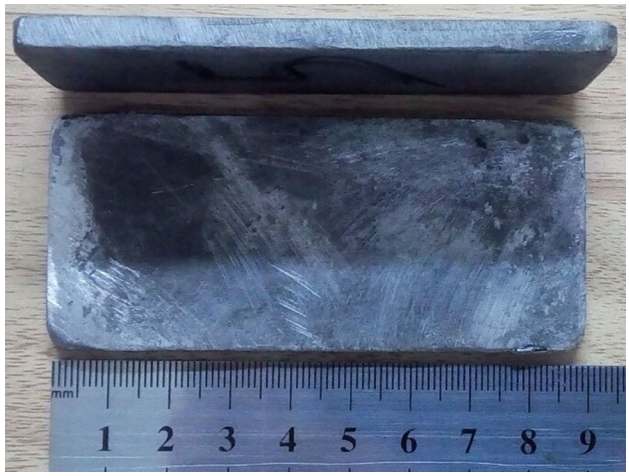

Fig. 2 Macroscopic photograph of the sample fabricated by hot pressing of powder

Optical microscopy (OM), scanning electron microscopy (SEM) and energy dispersive spectrophotometric (EDS) analysis were used to study the microstructure modification of the matrix and reinforcement distribution in the SiCp/Mg-9%Al nanocomposite introduced by hot pressing of powder assisted ultrasonic vibration under a semi-solid state. Samples for microstructure analysis were carried out in the central part of the specimens parallel to the pressing direction and were prepared by the conventional mechanical polishing. The interface bonding situation between SiC nanoparticles and matrix alloy was studied using transmission electron microscopy (TEM). Specimens for TEM were prepared by grinding-polishing the sample to produce a foil of 50 μm thickness followed by punching 3-mm-diameter disks. The disks were electro-polished with a twin-jet electro-polisher.

Tensile test was performed on a universal tensile machine at room temperature with the tensile rate of 0.5 mm/min. Four samples for repeat tensile tests were cut from each specimen, and the tensile strength reported in the present work was averaged from the four tensile tests.

3. Results and Discussion

3.1 Relative Density

The Archimedes drainage method was employed to measure the density of the composites. The relative density of the composites can be calculated by comparing the measured and the theoretical densities. The relative densities of the composites fabricated at different hot-pressing temperatures are shown in Fig. 3. It can be found the relative density increases steeply as the hot-pressing temperature varies from 450 to 510 °C.

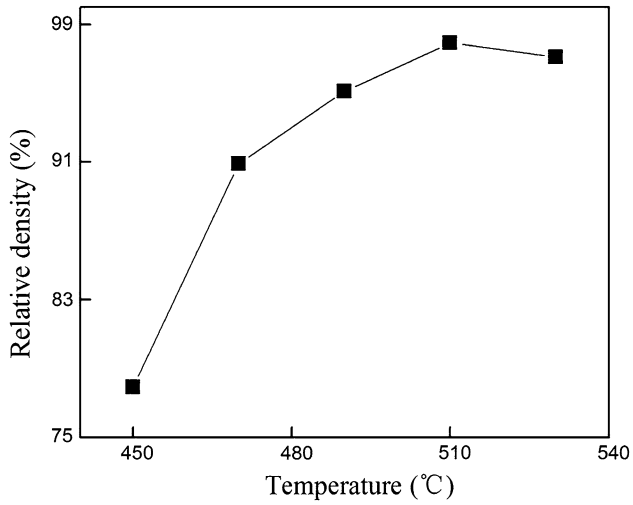

Fig. 3 Relative density of the composites

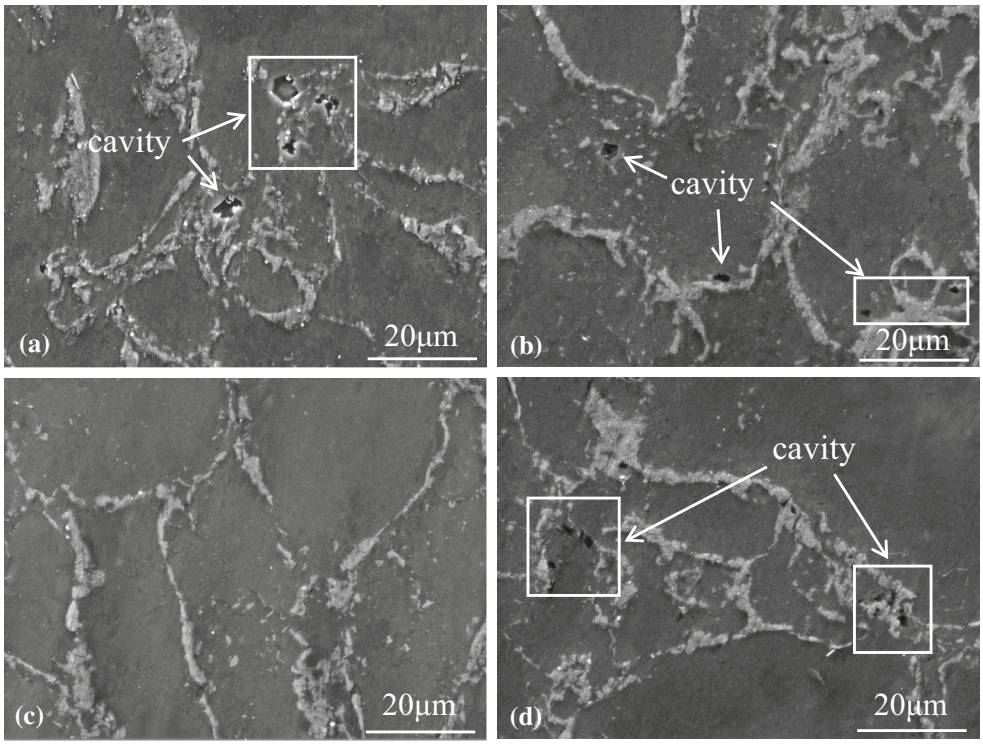

Fig. 4 SEM photographs of n-SiCp/Mg-9%Al composites fabricated at temperatures of (a) 450 °C, (b) 490 °C, (c) 510 °C and (d) 530 °C

Nevertheless, the relative density declines slightly at the hot-pressing temperature of 530 °C. This result is consistent with the microstructure of the composites as shown in Fig. 4. It illustrates that the hot-pressing temperature has a direct effect on the relative density of the nanocomposites. On the one hand, the elevated hot-pressing temperature accelerates the atomic diffusion between the particles and the combination between the powder (Ref 20). On the other hand, the matrix alloy can flow into the SiC particle clusters because the flow property improves as the hot-pressing temperature increases. Hence, the gas in the SiC particles clusters is gradually squeezed out, which contributes to the increase in relative density. However, the gas solubility in the melt increases as the temperature (Ref 21) and the liquid fraction in the matrix alloy increase, which leads to parts of gas adsorbed at the surface of powder dissolves in the melt before it is squeezed out from the nanocomposites. Consequently, the relative density of the nanocomposites declines slightly when the hot-pressing temperature rises to 530 °C.

3.2 Microstructure

Figure 5 shows the optical microstructures of n-SiCp/Mg-9%Al composites and the Mg-9%Al alloy. It can be clearly seen that the grain size of matrix as well as the agglomeration of n-SiCp in the n-SiCp/Mg-9%Al composites is gradually decreased as the hot-pressing temperature varying from 450 to 510 °C, while it is increased slightly when the hot-pressing temperature rises to 530 °C. Firstly, the solid metal powder becomes a semi-solid slurry as the hot-pressing temperature increases, which results in decreasing the agglomeration of n-SiCp. This result is attributed to the following reasons: (1) the semi-solid metal slurry with high viscosity and excellent fluidity is beneficial for improving the wettability and dispersibility of nanoparticles in the matrix (Ref 22) and (2) under the double effects of cavitation and acoustic streaming caused by ultrasonic vibration, the diffuse particle clusters in front of the liquid-solid interface can be resolved in the semi-solid slurry. Secondly, the dispersed SiC nanoparticles could hinder growth of the matrix grains by pinning grain boundaries. The triple effect of pressure, ultrasound and temperature can impact the nucleation and growth of primary crystals in the semi-solid slurry, so the homogeneity of the grain size distribution is improved. However, the volume fraction of the liquid phase in the semi-solid slurry increased from 30 to 50% when the temperature increased from 510 to 530 °C, and as a consequence, the agglomeration of SiC particles increased mildly due to the different densities of SiC and liquid Mg, which caused the deposition, floatation and segregation of SiC particles in the liquid (Ref 22). Moreover, the excessive temperature accelerated the growth of grain during solidification.

The Mg-9%Al alloy was fabricated under the same conditions as the nanocomposites with the hot-pressing temperature of 510 °C. Compared with the Mg-9%Al alloy, grains in all the nanocomposites are refined by the addition of SiC nanoparticles as shown in Fig. 5 for the reason that reinforcement particles below a certain size are pushed ahead of the solidification front in the semi-solid composites and can act to restrict grain growth during the solidification process (Ref 23). Figure 6 is the SEM micrographs and the result of EDS analysis of the nanocomposites fabricated at the temperature of 510 °C, and it can be seen that most of SiC nanoparticles segregate to the phase β-$Mg_{17}Al_{12}$ phase and some disperse uniformly in the matrix of the nanocomposites, indicating that the nanoparticles are largely distributed in the front of the liquid-solid interface

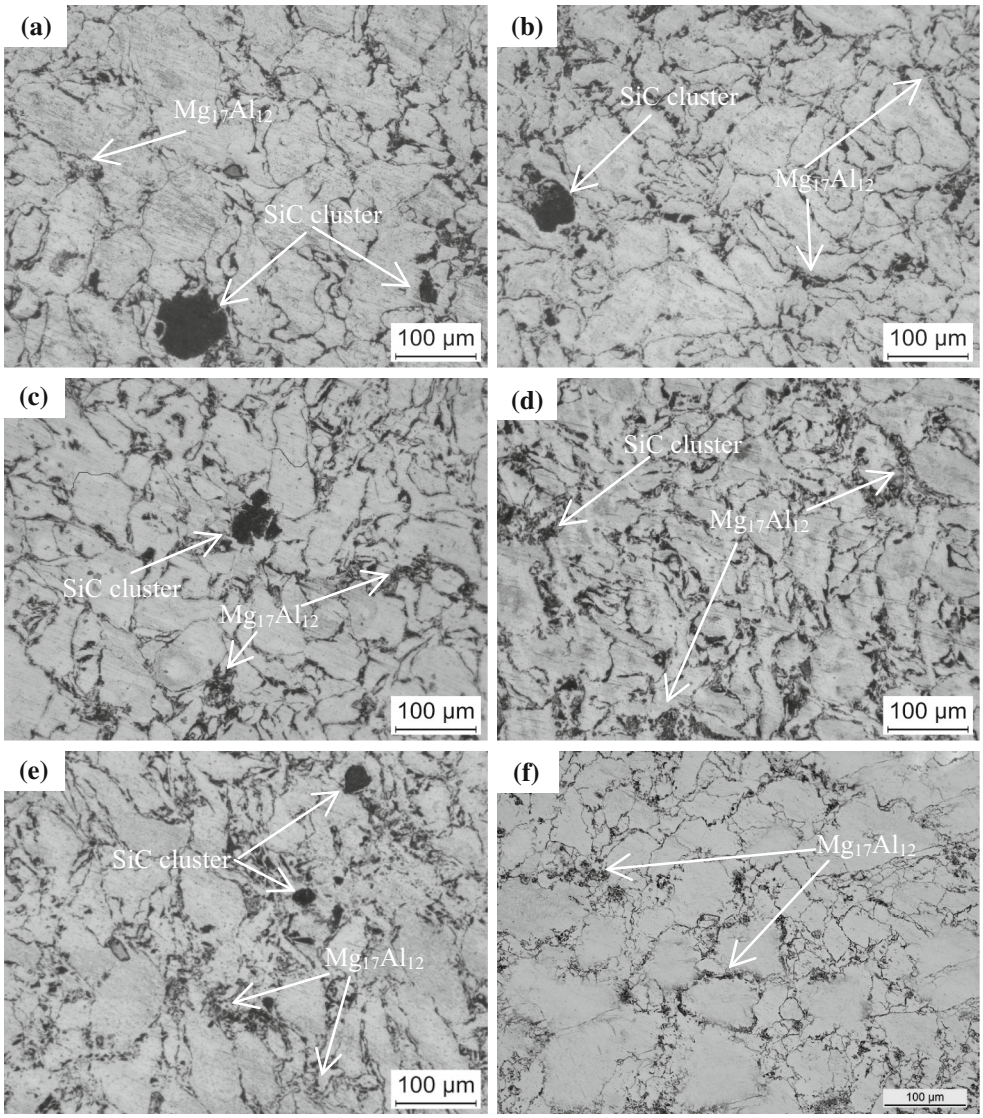

Fig. 5 OM micrographs of the n-SiCp/Mg-9%Al composites fabricated at the temperatures of (a) 450 °C, (b) 470 °C, (c) 490 °C, (d) 510 °C, (e) 530 °C and (f) the Mg-9%Al alloy fabricated at the temperature of 510 °C

during the growing of grains. This result could be attributed to the "push" effect of the solidification front on nanoparticles (Ref 23). On the one hand, the lower thermal conductivity of SiC nanoparticles affects the temperature gradient ahead of the solidification front and therefore acts as a barrier to the removal of the heat necessary for further solidification. On the other hand, the solid particle acts as a barrier preventing solute diffusion away from the tip of growing grains, thereby changing the concentration gradient and restricting growth. Thus, obvious agglomerates of SiC nanoparticles along grain boundaries are observed in the nanocomposites. This result indicates that the process parameters need further optimization in order to get rid of the remaining nanoparticle clusters, occurring mainly at the grain boundaries.

Figure 7 shows the TEM micrographs of SiC nanoparticles and EDS spectrum of phases in the SiCp/Mg-9%Al nanocomposites fabricated at the temperature of 510 °C. It can be seen that some of SiC nanoparticles are well dispersed while some are found to be agglomerated as shown in Fig. 7(a). As shown in Fig. 7(b), the results of EDS analysis of the regions marked in Fig. 7(a) demonstrate that the composition of the particle cluster is SiC nanoparticles, which are in agreement with the particle clusters as shown in Fig. 5. It can be clearly seen that the interfacial bonding between the SiC nanoparticles and the Mg-9%Al matrix is very well and no microcracks appear.

3.3 Tensile Properties

Figure 8 shows the yield strength (σ_{YS}, 0.2% proof stress), ultimate tensile strength (σ_{UTS}, the ultimate tensile strength) and elongation to fracture of the Mg-9%Al alloy and SiCp/Mg-9%Al nanocomposites fabricated by hot pressing of powder assisted ultrasonic vibration at different temperatures. It can be seen in Fig. 8(a) that the yield strength, ultimate tensile strength and elongation to fracture of the SiCp/Mg-9%Al nanocompos-

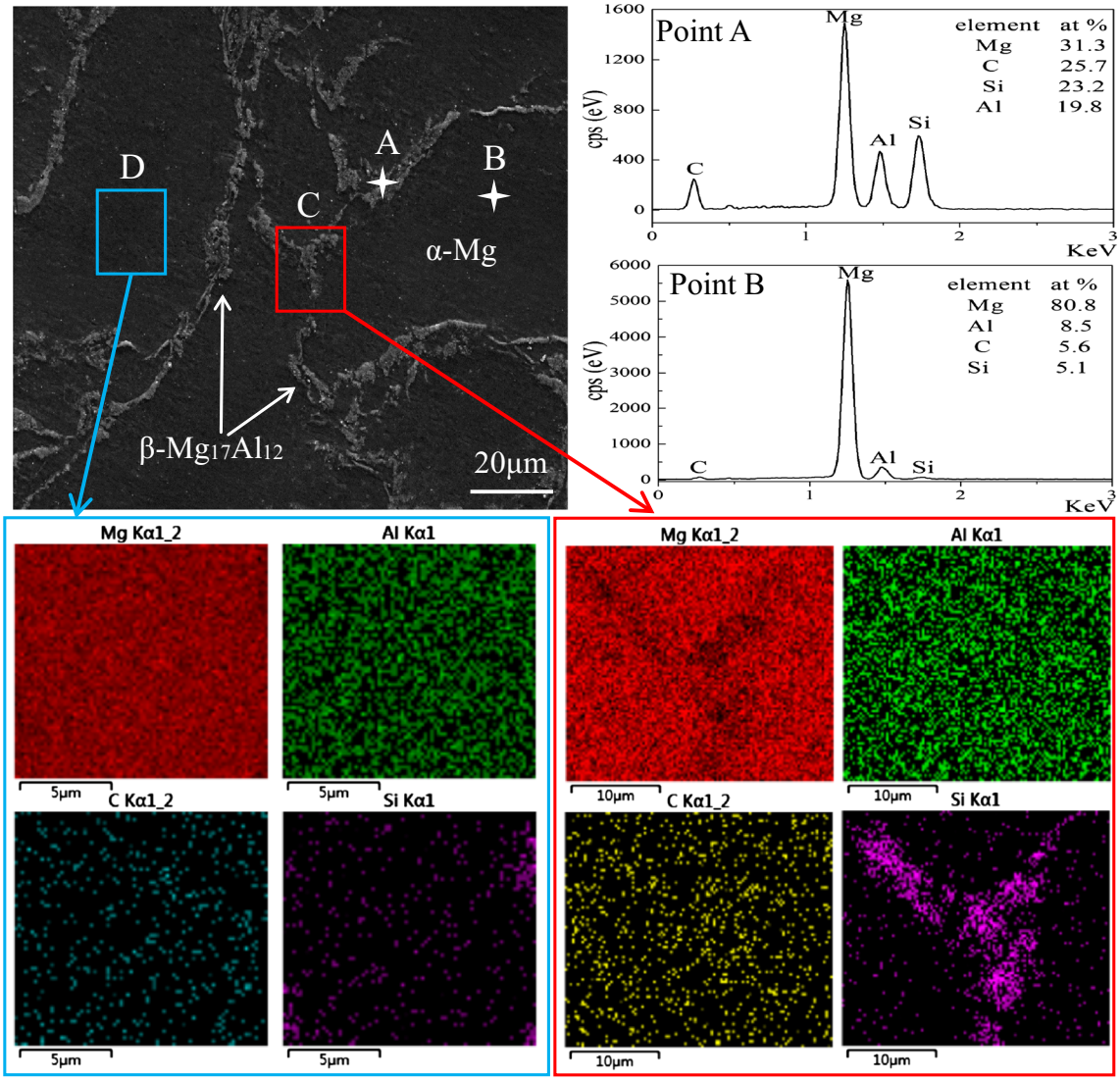

Fig. 6 SEM micrograph and EDS analysis result of the n-SiCp/Mg-9%Al composites fabricated at the temperature of 510 °C

ites increased obviously with the increase in hot-pressing temperature from 450 to 510 °C and then decreased significantly when the hot-pressing temperature increased to 530 °C. This observation can be attributed to the porosity of the nanocomposites and the distribution of SiC nanoparticles in the nanocomposites. Indeed, Tekmen et al. (Ref 24) reported that the increase in porosity content decreases both the yield and ultimate tensile strength values of the produced samples. In the present study, compared to other samples prepared at different temperatures, the samples fabricated at 510 °C have the optimal relative density and the most uniform particle distribution. Therefore, the samples fabricated 510 °C have the optimal tensile properties.

As shown in Fig. 8, the yield strength, ultimate tensile strength and elongation to fracture of the SiCp/Mg-9%Al nanocomposites are improved by 53.4, 39.8 and 104.3%, respectively, compared with the Mg-9%Al alloy. According to the classic Hall-Petch equation:

$$\sigma_y = \sigma_0 + K_y d^{-1/2} \quad \text{(Eq 1)}$$

where σ_y is the yield strength, σ_0 and K_y are material constants, and d is the mean grain size, the YS of a given alloy is proportional to $d^{-1/2}$. Therefore, the grains of the nanocomposites are refined gradually by the addition of SiC nanoparticles, as discussed in section 3.2, which can contribute to the increase in yield strength. Additionally, the contribution by the Orowan strengthening ($\Delta\sigma_{Orowan}$) mechanism included by well-dispersed nanoparticles, as shown in Fig. 7(a), can be calculated by the following equation (Ref 1):

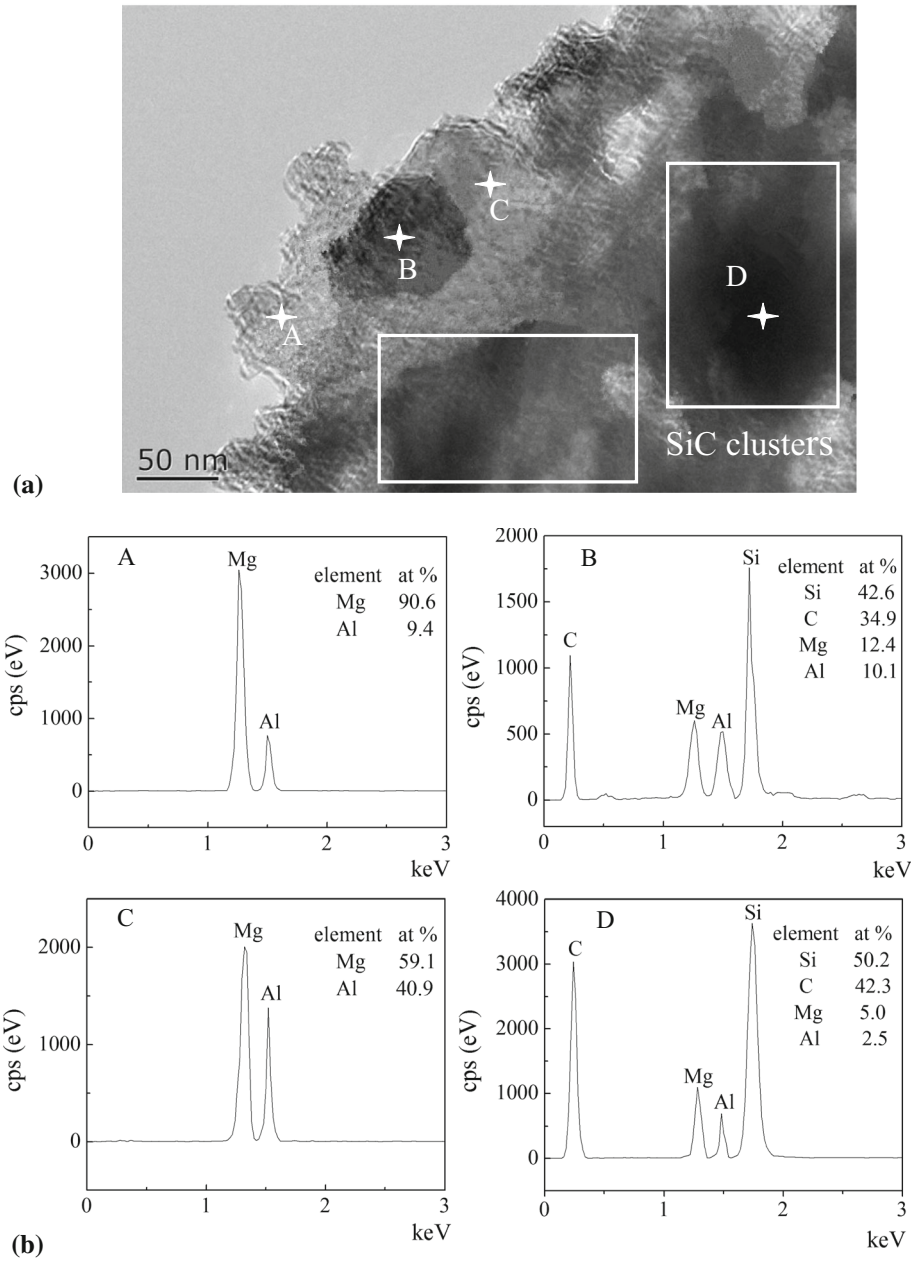

Fig. 7 TEM micrographs (a) and EDS spectrum of phases (b) in the SiCp/Mg-9%Al nanocomposites fabricated at the temperature of 510 °C

$$\Delta\sigma_{\text{Orowan}} = \frac{\varphi G_{\text{m}} b}{d_{\text{p}}} \left(\frac{6V_{\text{p}}}{\pi}\right)^{1/3} \quad \text{(Eq 2)}$$

where G_{m}, b, V_{p} and d_{p} are the shear modulus of the matrix, the Burgers vector, the volume fraction and the size of the nanoparticles uniformly dispersed in the composites, respectively. φ is a constant.

It can be further concluded that obvious grain refinement and the Orowan strengthening mechanism should play a major role in the enhancement of the tensile properties of the nanocomposites in our work.

Figure 9 shows the fracture surface of SiCp/Mg-9%Al nanocomposites fabricated by hot pressing of powder assisted ultrasonic vibration at different temperatures. For the n-SiCp/Mg-9%Al composites fabricated at temperatures of 450, 470

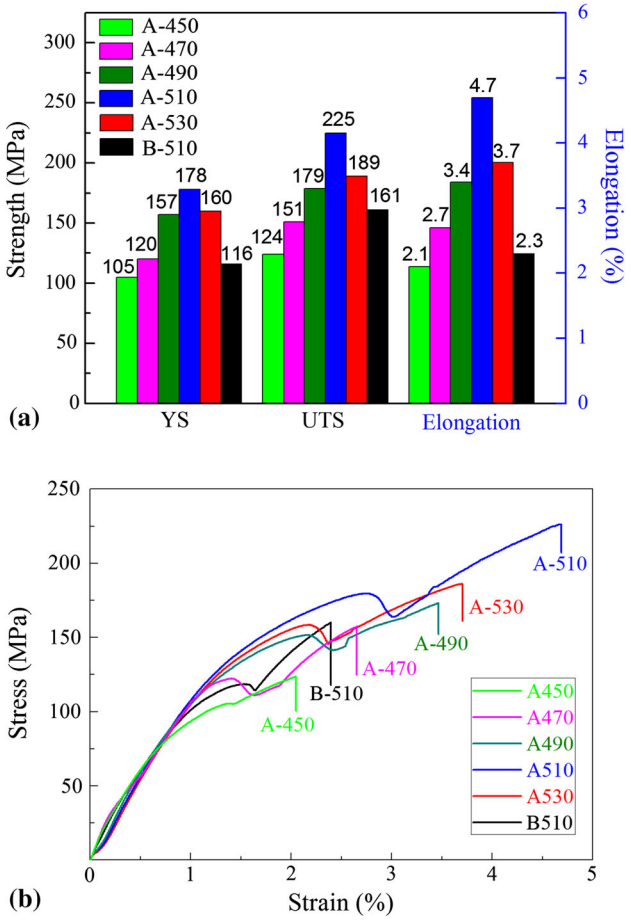

Fig. 8 Tensile properties of Mg-9%Al and its composites. (a) Typical tensile stress-strain curves and (b) YS, UTS and elongation

and 490 °C, the fracture surface is smooth. By the further magnification, a few agglomerated SiC particulates and microvoids are found in the n-SiCp/Mg-9%Al composites, as shown in Fig. 9(a), (b) and (c). As the hot-pressing temperature increases, the amount of microvoids decreases while the amount of dimples increases. However, some microvoids exist in the n-SiCp/Mg-9%Al composites when the hot-pressing temperature increases to 530 °C. This result is consistent with the microstructure of the composites, which is shown in Fig. 4.

The relationship between particle strength and particle/matrix interfacial bonding strength is a critical criterion to determine the type of fracture in the composites during deformation (Ref 25). For the SiC reinforced composite, large stress concentrations will occur at the interface of SiC/Mg owing to the deformation incompatibility between the hard particles and soft Mg matrix. Once the stress is larger than the interfacial bonding strength, microcracks might occur at the interface of SiC/Mg. The number of agglomerated SiC particulates and microvoids in the SiCp/Mg-9%Al nanocomposites fabricated at 510 °C is the lowest among other samples, as shown in Fig. 4 and 9. Hence, it can be concluded that the n-SiCp/Mg-9%Al composites fabricated at the hot-pressing temperature of 510 °C achieved the optimal tensile properties. The fracture observations are consistent with the results shown in Fig. 8.

4. Conclusion

Magnesium matrix composites reinforced with SiC nanoparticles have been successfully fabricated by hot pressing of powder assisted ultrasonic vibration under a semi-solid state. The microstructures and tensile properties of n-SiCp/Mg-9%Al composites were experimentally investigated.

1. The relative density increases steeply as the hot-pressing temperature varying from 450 to 510 °C. Nevertheless, it declines slightly at the hot-pressing temperature of 530 °C.
2. With increasing the hot-pressing temperature from 450 to 510 °C, the grains are gradually refined and the agglomeration of the n-SiCp is evidently reduced. Most of the n-SiCp are distributed along grain boundaries in the nanocomposites, while some dispersed n-SiCp are inside the grains of matrix in the n-SiCp/Mg-9%Al composites.
3. The n-SiCp/Mg-9%Al composites fabricated at the hot-pressing temperature of 510 °C achieved the optimal mechanical properties. The ultimate tensile strength, yield strength and elongation to fracture of the nanocomposites were improved by 53.4, 39.8 and 104.3%, respectively,

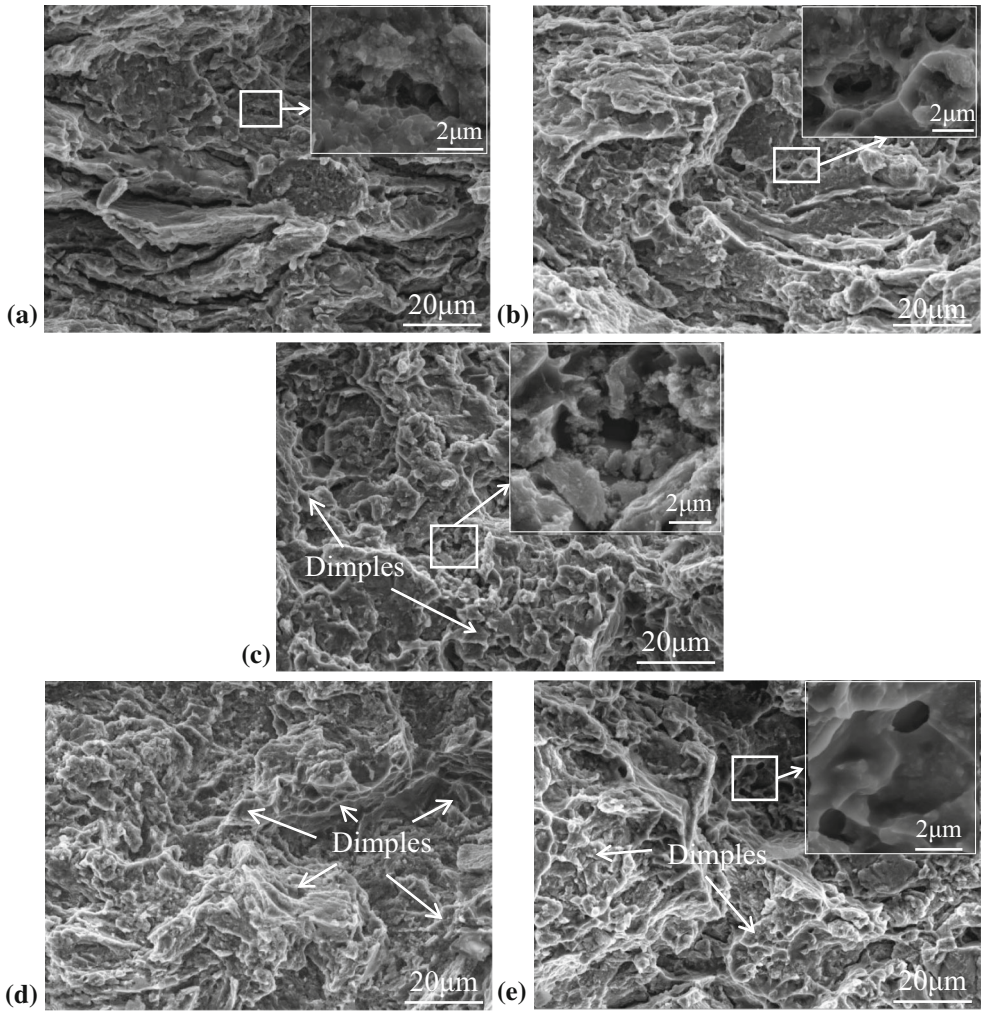

Fig. 9 Fracture surface of n-SiCp/Mg-9%Al composites fabricated at the temperatures of (a) 450 °C, (b) 470 °C, (c) 490 °C, (d) 510 °C and (e) 530 °C

compared with that of the Mg-9%Al alloy. This improvement could be attributed to obvious grain refinement and the Orowan strengthening mechanism.

Acknowledgments

The authors gratefully acknowledge the financial support obtained from the National Natural Science Foundation of China (Grant Nos. 51301118 and 51401144), the Projects of International Cooperation in Shanxi (Grant No. 2014081002) and Technological Innovation Programs of Higher Education Institutions in Shanxi (Grant No. 2013108).

References

1. L.Y. Chen, J.Q. Xu, H. Choi, M. Pozuelo, X.L. Ma, S. Bhowmick, J.M. Yang, S. Mathaudhu, and X.C. Li, Processing and Properties of Magnesium Containing a Dense Uniform Dispersion of Nanoparticles, *Nature*, 2015, **528**, p 539–543
2. F. Mirshahi and M. Meratian, High Temperature Tensile Properties of Modified Mg/Mg_2Si In Situ Composite, *Mater. Des.*, 2012, **33**, p 557–562
3. B. Çiçek, H. Ahlatçı, and Y. Sun, Wear Behaviours of Pb Added Mg-Al-Si Composites Reinforced with In Situ Mg_2Si Particles, *Mater. Des.*, 2013, **50**, p 929–935
4. R. Anish, M. Sivapragash, and G. Robertsingh, Compressive Behaviour of SiC/ncsc Reinforced Mg Composite Processed Through Powder Metallurgy Route, *Mater. Des.*, 2014, **63**, p 384–388
5. K.B. Nie, X.J. Wang, K. Wu, X.S. Hu, and M.Y. Zheng, Development of SiCp/AZ91 Magnesium Matrix Nanocomposites Using Ultrasonic Vibration, *Mater. Sci. Eng. A*, 2012, **540**, p 123–129
6. S.S. Zhou, K.K. Deng, J.C. Li, S.J. Shang, W. Liang, and J.F. Fan, Effects of Volume Ratio on the Microstructure and Mechanical Properties of Particle Reinforced Magnesium Matrix Composite, *Mater. Des.*, 2014, **63**, p 672–677
7. A. Das and S.P. Harimkar, Effect of Graphene Nanoplate and Silicon Carbide Nanoparticle Reinforcement on Mechanical and Tribological Properties of Spark Plasma Sintered Magnesium Matrix Composites, *J. Mater. Sci. Technol.*, 2014, **30**, p 1059–1070
8. C.S. Goh, J. Wei, L.C. Lee, and M. Gupta, Properties and Deformation Behaviour of Mg-Y_2O_3 Nanocomposites, *Acta Mater.*, 2007, **55**, p 5115–5121
9. G. Garcés, E. Oñorbe, P. Pérez, I.A. Denks, and P. Adeva, Evolution of Internal Strain During Plastic Deformation in Magnesium Matrix Composites, *Mater. Sci. Eng. A*, 2009, **523**, p 21–26

10. S.C.V. Lim and M. Gupta, Enhancing Modulus and Ductility of Mg/SiC Composite Through Judicious Selection of Extrusion Temperature and Heat Treatment, *Mater. Sci. Technol.*, 2003, **19**, p 803–808
11. K.B. Nie, X.J. Wang, K. Wu, M.Y. Zheng, and X.S. Hu, Effect of Ultrasonic Vibration and Solution Heat Treatment on Microstructures and Tensile Properties of AZ91 Alloy, *Mater. Sci. Eng. A*, 2011, **528**, p 7484–7487
12. K.K. Deng, C.J. Wang, X.J. Wang, K. Wu, and M.Y. Zheng, Microstructure and Elevated Tensile Properties of Submicron SiCp/AZ91 Magnesium Matrix Composite, *Mater. Des.*, 2012, **38**, p 110–114
13. K.B. Nie, X.J. Wang, X.S. Hu, L. Xu, K. Wu, and M.Y. Zheng, Microstructure and Mechanical Properties of SiC Nanoparticles Reinforced Magnesium Matrix Composites Fabricated by Ultrasonic Vibration, *Mater. Sci. Eng. A*, 2011, **528**, p 5278–5282
14. V. Viswanathan, T. Laha, K. Balani, A. Agarwal, and S. Seal, Challenges and Advances in Nanocomposite Processing Techniques, *Mater. Sci. Eng. R*, 2006, **54**, p 121–285
15. M. Habibnejad-Korayem, R. Mahmudi, and W.J. Poole, Enhanced Properties of Mg-Based Nano-Composites Reinforced with Al_2O_3 Nano-Particles, *Mater. Sci. Eng. A*, 2009, **519**, p 198–203
16. C.S. Goh, J. Wei, L.C. Lee, and M. Gupta, Development of Novel Carbon Nanotube Reinforced Magnesium Nanocomposites Using the Powder Metallurgy Technique, *Nanotechnology*, 2006, **17**, p 7–12
17. K.B. Nie, X.J. Wang, K. Wu, L. Xu, M.Y. Zheng, and X.S. Hu, Processing, Microstructure and Mechanical Properties of Magnesium Matrix Nanocomposites Fabricated by Semisolid Stirring Assisted Ultrasonic Vibration, *J. Alloys Compd.*, 2011, **509**, p 8664–8669
18. K.B. Nie, X.J. Wang, L. Xu, K. Wu, X.S. Hu, and M.Y. Zheng, Effect of Hot Extrusion on Microstructures and Mechanical Properties of SiC Nanoparticles Reinforced Magnesium Matrix Composite, *J. Alloys Compd.*, 2012, **512**, p 355–360
19. R.W. Hamilton, Z. Zhu, R.J. Dashwood, and P.D. Lee, Direct Semi-Solid Forming of a Powder SiC–Al PMMC: Flow Analysis, *Compos. Part A Appl. Sci. Manuf.*, 2003, **34**, p 333–339
20. X.P. Luo, M.G. Zhang, C.X. Lv, and X.X. Lv, Fabrication of Palladium-Free Nickel-Coated Carbon Fiber Reinforced Magnesium Alloy Composites by Powder Metallurgy Hot Extrusion and Their Microstructure, *Rare Met. Mater. Eng.*, 2012, **04**, p 0743–0747 ((in Chinese))
21. S. Gao and G.C. Yao, Research on Porosity of Carbon Fiber Reinforced Aluminum Matrix Composites, *Mater. Rev.*, 2006, **20**, p 462–464 ((in Chinese))
22. Y. Sun and Z.H. Chen, Research Status of Rheological Behavior and Production of Semi-Solid Forming Metal Matrix Composites, *Mater. Rev.*, 2005, **03**, p 56–59 ((in Chinese))
23. B.F. Schultz, J.B. Ferguson, and P.K. Rohatgi, Microstructure and Hardness of Al_2O_3 Nanoparticle Reinforced Al-Mg Composites Fabricated by Reactive Wetting and Stir Mixing, *Mater. Sci. Eng. A*, 2011, **530**, p 87–97
24. C. Tekmen, I. Ozdemir, U. Cocen, and K. Onel, The Mechanical Response of Al/Si/Mg/SiCp Composite: Influence of Porosity, *Mater. Sci. Eng. A*, 2003, **360**, p 365–371
25. H.S. Chen, W.X. Wang, Y.L. Li, J. Zhou, H.H. Nie, and Q.C. Wu, The Design, Microstructure and Mechanical Properties of B_4C/6061Al Neutron Absorber Composites Fabricated by SPS, *Mater. Des.*, 2016, **94**, p 360–367